Uncovering the Neural Fingerprint of Akinetic States in a Parkinson's Disease Rodent Model

Elisa L. Garulli[1*], Timon Merk[2], Ghadi El Hasbani[1], Burçe Kabaoğlu[1], Rafael De Sa[1], Ruben Behrsing[1], Dennis Doll[8, 11], Michael Schellenberger[8], Arend Vogt[1, 10], Wolf-Julian Neumann[2], Yangfan Peng[10], Matthias Endres[3, 4, 5, 6, 9], Christoph Harms[1,3,4,7], Nikolaus Wenger[1*]

***For correspondence:** nikolaus.wenger@charite.de (NW); elisa.garulli@charite.de (ELG)

Present address: [§]Department, Institute, Country; [¶]Department, Institute, Country

[1]Department of Experimental Neurology, Charité – Universitätsmedizin Berlin; [2]Movement Disorders Unit, Charité - Universitätsmedizin Berlin, Berlin, Germany; [3]Center for Stroke Research Berlin, Charité-Universitätsmedizin Berlin; [4]DZHK (German Center for Cardiovascular Research), Berlin, Germany.; [5]DZNE (German Center for Neurodegenerative Diseases), Berlin, Germany.; [6]DZPG (German Center of Mental Health), Berlin, Germany.; [7]Einstein Centre for Neuroscience Berlin; [8]Institute of Clinical Neurobiology, University Hospital Wuerzburg, Wuerzburg, Germany; [9]Klinik und Hochschulambulanz für Neurologie, Charité-Universitätsmedizin Berlin; [10]Department of Neurology and Neuroscience Research Center, Charité – Universitätsmedizin Berlin; [11]Indoc Research Europe gGmbH, Mainz, Germany

Abstract Parkinson's Disease (PD) is characterized by complex motor deficits, including transient akinetic episodes during locomotion. Here, we investigated the neural correlates of akinesia in a 6-OHDA rat model of PD. We developed the open-source toolbox *neurokin* to analyse the kinematic and neural signal recorded during a runway task. First, we observed that compared to control, PD rats spent significantly more time in akinetic episodes, which were correlated with an increase in beta-band power. Next, we computed a set of temporally resolved kinematic and neural features capturing the evolution of locomotion states. We employed linear and non-linear machine learning models, to retrieve salient features that characterized akinetic episodes. Beyond confirming established associations with beta power, we identified Hjorth complexity and mobility as time-domain features modulated by akinetic onset. Our findings highlight novel, computationally lightweight biomarkers that might serve as targets for future state-adaptive neuromodulation therapies.

Introduction

Animals exercise volition through various movements in space (***Kranick and Hallett 2013***). Among these, *locomotion* is the sequence of behaviours performed to change location (***Latash 2012***). A locomotion sequence includes *gait*, which is the cyclical limb movements required to propel the animal forward (***Kiehn 2016***), and can be preceded, interrupted or followed by active or inactive behaviours (***Nishimaru et al. 2023***). Active motor behaviours include grooming, sniffing, and scanning the environment - here collectively referred to as *stationary movement*. Inactive motor behaviours include freezing, a state of akinesia that can occur as an innate response to acute stressors (***Tovote***

2024), or as a pathological symptom of neurological disorders (*Nutt et al. 2011*). In this study, we investigated three distinct behavioural states within the locomotion sequence of a 6-OHDA rodent model of Parkinson's Disease (PD): *gait* (cyclical limb movement to achieve forward progression), *stationary movement* (active behaviours without forward displacement) and *akinesia* (complete immobility). In particular, we focused on characterizing the state of *akinesia*, as a manifestation of Parkinson's disease (*Xiao et al. 2017*).

PD is a neurodegenerative disease characterized by a diverse array of neural and phenotypical symptoms, ranging from emotional components to motor deficits (*Martínez-Fernández et al. 2016*, *Weintraub and Burn 2011*). Motor symptoms encompass a variety of deficits, such as hypo- and bradykinesa (little or slow movement), tremor, and Freezing of Gait (FoG). FoG is described as *"brief, episodic absence or marked reduction of forward progression of the feet, despite the intention to walk"* by *Nutt et al. 2011*. Current PD-therapies include dopaminergic medication, eventually combined with Deep Brain Stimulation (DBS) primarily of the Subthalamic Nucleus (STN). These interventions are effective at addressing tremor and rigidity but can lead to side effects (*Pötter-Nerger and Volkmann, 2013*), and have moderate, or null, efficacy on axial symptoms such as FoG (*Castrioto, 2011*). The limitations of pharmaceutical and open-loop neuromodulation, led to the exploration of adaptive DBS protocols to provide personalized improvements (*Oehrn et al., 2024*). An effective adaptive protocol hinges on identifying suitable biomarkers that correlate with symptoms and can be monitored to guide the intervention.

The beta band oscillation (13-35 Hz in humans) is a common target for adaptive DBS as it correlates with motor deficits (*Tinkhauser et al., 2017*). Indeed, algorithms locking to beta bursts (*Little et al. 2013*, *Tinkhauser et al. 2017*) showed promising results, and phase-locked stimulation (*McNamara et al., 2022*) has recently been proposed as a further refinement. Despite the crucial role of beta band in PD, it is not certain that this biomarker will be optimal for every patient, which invites the exploration of other neural correlates (*Neumann et al. 2023*). Recently, gamma power entrainment has also shown to be effective in ameliorating a diverse set of motor symptoms (*Oehrn et al., 2024*). Discovering novel biomarkers, in addition to the current targets, can pave the way to further personalize stimulation protocols (*Oliveira et al., 2023*). Moreover, the combination of multiple neural markers, in a model-based fashion (*Little and Brown, 2012*) is a promising strategy to address complex symptomatic manifestations (*Neumann et al. 2019*, *Little and Brown 2012*). This brings the implication that the selected biomarkers should come with low computational cost and lag, providing valuable insights in the neural states without delaying the intervention (*Little and Brown, 2012*).

While some neural correlates of locomotion deficits have been characterized in humans (*Toledo et al. 2014*, *Shine et al. 2014*), animal models of PD offer a solid platform to explore motor impairments and inform the next generation of neuromodulation therapies (*Wenger et al., 2022*).

To relate the symptoms of rodents with those of patients, it is crucial to collect rich datasets that allow the exploration of pathological manifestations at multiple levels. To address this need we developed *neurokin*, an open-source and beginner-friendly package to ease the import and processing of invasive neural and kinematic data. Here, we showcase its utility to investigate motor deficits in a Parkinson's model and refine the quantification of known neural-correlates.

Further, we set to investigate the neural fingerprints of akinetic states during locomotion to reveal novel correlates. We used *py_neuromodulation* (*Merk et al., 2023*), a toolbox for standardized electrophysiological data processing, to extract neural features and *neurokin* to compute kinematic features, creating a multimodal dataset that captures the neurobehavioural evolution of locomotion states with high temporal precision. Next, we used machine-learning models to explore the salient features that best characterize the akinetic state. Finally, we identified promising new parameters that correlate with akinetic episodes onset, thus potentially expanding the available targets for next-generation stimulation protocols. We explored both frequency- and time-domain features, specifically highlighting Hjorth complexity (deviation from a sinusoid), mobility (frequency variance) and activity (power variance) (*Hjorth 1970*). These parameters are computationally efficient and

low-latency, making them attractive target candidates for closed-loop neuromodulation.

Results

neurokin enables the temporal and neural characterization of locomotion states

We used *neurokin*, to confirm disease-specific neurobehavioural deficits in the PD model compared to sham controls. To create a reproducible rodent model, the neurotoxin 6-hydroxydopamine (6-OHDA) was unilaterally injected into the left Medial Forebrain Bundle in N=6 Sprague Dawley rats, resulting in the degeneration of dopaminergic innervation (**Fig 1a**). The degeneration was evaluated through Tyrosine Hydroxylase (TH) staining and imaging of axonal projections in the Striatum (**Fig 1b**), with quantification achieved by comparing fluorescence signal intensity between the two hemispheres (left hemisphere mean signal: 4.78 $\pm$0.51, right hemisphere mean signal: 30.41 $\pm$4.22, $P < 0.001$) (**Fig 1c**). To test neurobehavioural deficits, we collected primary motor cortex (M1) ElectroCorticoGraphy (ECoG) signals (at a sampling rate of 24K Hz) while the animals behaved freely on the runway and video recorded the experiments (at a 50 Hz frame rate). From the videos, we manually labelled the three locomotion states: gait, stationary movement and akinesia - thus establishing the events ground truth (**Fig 1d**). A representative labelling is displayed in **Video Supplement 1**.

We used *neurokin* to convert the manual labels in timestamps and synchronize the events to the neural data (**Fig 1e**). We then built a pipeline to compute the percentage of time spent in each state and the subject-level statistics. The analysis found that rats injected with 6-OHDA spent more time in akinetic states ($P < 0.01$, t-test with Bonferroni-Holm correction) and less time in gait than sham rats ($P < 0.05$, t-test with Bonferroni-Holm correction) (**Fig 1f**). Next, we expanded the pipeline to neural data and calculated the corresponding Power Spectral Density (PSD) between 5 and 100 Hz of M1 ECoG signals of the 6-OHDA model animals (**Fig 1g**). Restricting the power spectrum to the established frequency of beta in the rodent model (20-42 Hz, ***Brazhnik et al. 2014***) we identified a distinct modulation of the beta band across the locomotion states, highlighting an increased beta band activity specifically during states of akinesia, compared to stationary movement ($P < 0.001$) and gait ($P < 0.001$) (**Fig 1h**). We modelled the group comparison using a Linear Mixed Model, setting the event type as the fixed effect and the day of recording nested within the subject variable as the random effect.

These results validated and quantified previous findings showing 6-OHDA rats exhibited prolonged akinesia compared to shams (***Xiao et al., 2017***), and further elucidated the correlation between the beta band and the presence of motor symptoms (***Degos et al., 2009***). The presence of the akinetic state in the PD rats, together with the substantial increase in beta band power during akinetic episodes, indicated a pathogenic characteristic of this state.

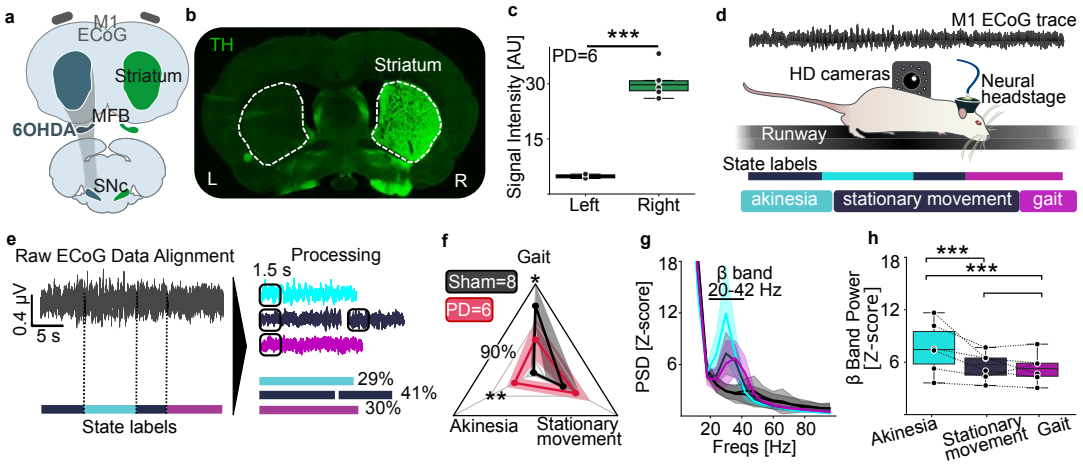

Figure 1. Neurobehavioural characteristics of the PD rodent model

a. Parkinson's model scheme. Unilaterally 6-OHDA-injected rats were implanted with ECoG electrodes over the Motor Cortex. **b. Tyrosine-Hydroxylase (TH) staining** of the dopaminergic neurons' projection to the Striatum highlighted a successful unilateral degeneration in the injected side (left). **c. Quantification of the TH staining** confirmed a consistent degeneration of dopaminergic neurons **d. Behaviour experiment set-up.** Rats were trained to walk on a runway. Their movements were recorded with a marker-based recording set-up, and the neural data were acquired with a headstage. Locomotion states were identified with an offline video-based analysis. **e. Overview of the modular pipeline enabled by neurokin.** We built a pipeline with two *neurokin* modules to characterize locomotion states. We converted manually-placed timestamps in time percentages and calculated their distribution. Then, we synchronized the neural data and compute the PSD values corresponding with the locomotion states. **f. Distribution of locomotion states.** The percentage of time spent in each state revealed a significant increase in akinesia ($P < 0.01$) and a reduction in gait ($P < 0.05$) for PD animals (red) compared to sham (black), shaded areas indicate standard deviation. **g. Spectral analysis of locomotion states.** Analysis of the neural correlates of locomotion states confirmed a characteristic increase of the beta band specifically during the state of akinesia (cyan), in respect to stationary movement (dark purple), gait (magenta), and sham animals (black, the akinetic trace was omitted as the number of available episodes was insufficient). **h. Linear Mixed Model analysis.** We modelled the event type as the fixed effect in an LMM considering the experiment day nested within the subject as the random effect. The amplitude of the beta band (20-42 Hz) was significantly increased during states of akinesia ($P < 0.001$ compared to stationary movement, $P < 0.001$ compared to gait).)

Linear model reveals neurokinematic feature contributing to states separation

To expand on these initial findings, we sought to expand our understanding of the neural correlates of akinesia in the context of locomotion. To this end, we created a multimodal dataset, synchronizing 36 kinematic features (from 3D coordinates recorded at 200 Hz) and 108 neural features sampled at 200 Hz (please refer to **Suppl. Table 1** for the full list of features used). Thus, the identical 5 ms interval may be examined from both a "kinematic perspective" and a "neural perspective". We used *neurokin* to extract kinematic features from the 3D coordinates recorded from infrared (IR) cameras, and *py_neuromodulation* for estimating the features of ECoG data (***Merk et al. 2023***)(**Fig 2a**). Initially, we analysed the dataset using Linear Discriminant Analysis (LDA). We developed two models, utilizing either the kinematic or the neural portion of the multimodal dataset.

As a proof of principle, we computed the LDA model using solely the kinematic features to establish if any discriminating features could be retrieved. Intuitively, the model could separate the gait state, but confounded the stationary movement with the akinetic state (**Fig 2b**). To understand which features contributed the most to the state separation, we inspected the model with a permutation feature importance test. We repeated the test in a cross-validation design, leading to the identification of the top 5 features (**Fig 2c**). Intuitively, the features that contributed the most to the separation of the states, represented the linear speed of different joints. We visually inspected the directionality of these features by plotting the corresponding scaling on the LDA space. This confirmed that high values in speed-related variables correlated with the direction of separation of the gait state (**Fig 2d**). Finally, we quantified the performance of the model in predicting the state values of unseen data, within a cross-validation (f1-score: 0.69), and computed the average confusion matrix (**Fig 2e**). We grouped the categories of akinesia and stationary movement, as we expected the kinematics-based model not to be able to meaningfully differentiate the two states (**Suppl. Fig 1a** displays the expanded 3x3 confusion matrix). In line with the projection, the LDA model could separate akinesia and stationary movement (97% $\pm$3% true positive) from the gait state (62% $\pm$14% True positive rate).

After validating this approach on the kinematic features, we repeated the same steps using the neural portion of the dataset. The model confounded the states of stationary movement and gait but could separate the state of akinesia to a better degree than the kinematic-based model (**Fig 2f**). We computed the most relevant neural features (**Fig 2g**), and retrieved known akinetic correlates (i.e., features related to the beta band ***Brown 2007***), and known prokinetic correlates (gamma band amplitude ***Litvak et al. 2012***). Moreover, we uncovered Hjorth complexity and mobility as potential novel neural correlates of akinesia (***Hjorth 1970***). Projecting the loadings in the LDA space (**Fig 2h**), suggests that Hjorth complexity in the left hemisphere (6-OHDA injected) correlates with akinetic episodes while Hjorth mobility on the right hemisphere correlates with movement. Finally, we quantified the performance of the model in predicting the state of unseen data (f1-score:0.64), and computed the average confusion matrix (**Fig 2i**). Here, we grouped the categories of stationary movement and gait as our focus was the neural distinction between the akinetic state versus active states (**Suppl. Fig 1b** displays the expanded 3x3 confusion matrix). Indeed the model returned a complementary result to the kinematic model: the akinetic state was distinguished above chance level (56% $\pm$11%) from the active states of gait and stationary movement (82% $\pm$6%).

These results suggest that the akinetic state has a distinct fingerprint in its neural correlates, which is not limited to the beta band.

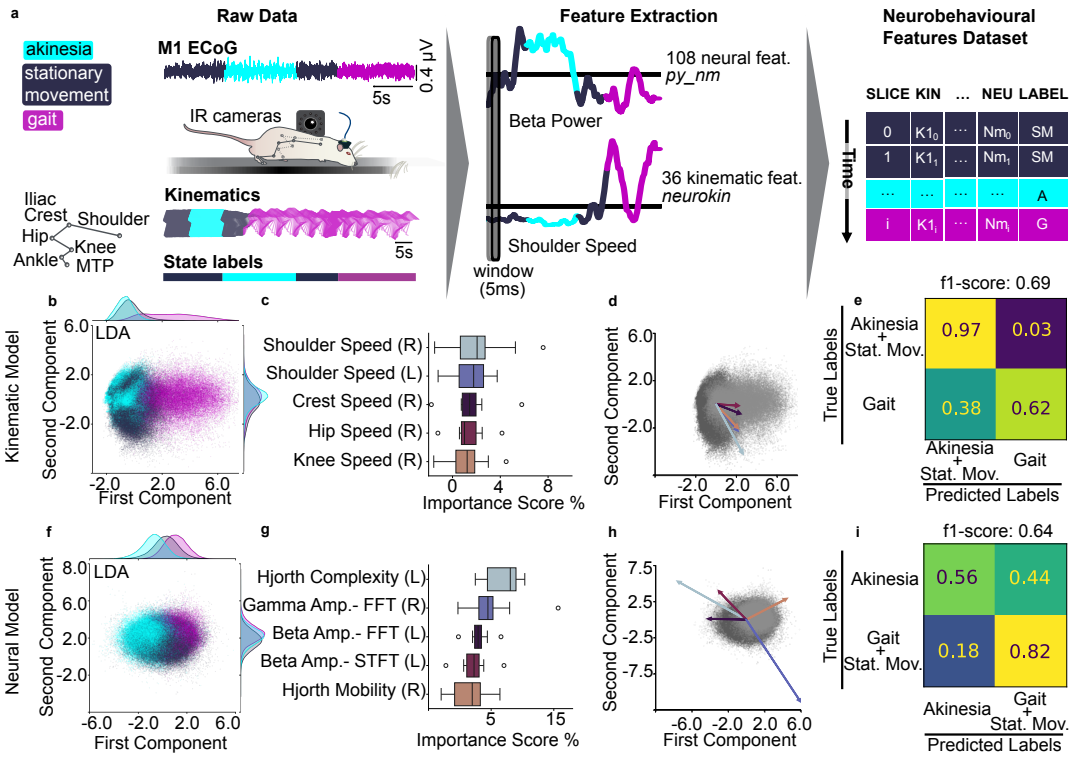

Figure 2. Linear model reveals feature contributing to states separation

a. Feature extraction paradigm. Synchronized kinematic and neural data were collected from rats walking on a runway. Locomotion events were labelled offline, 3D bodyparts coordinates were extracted from infrared (IR) cameras. We used *py_neuromodulation* to compute 108 neural features (e.g., oscillatory, temporal waveform-shape, spectral parametrization) and *neurokin* to compute 36 kinematic features (e.g., angles, speed, velocity). The final dataset includes synchronized neurobehavioural features. **b. LDA using kinematic features.** Using features computed from the 3D coordinates, points belonging to the gait state were noticeably separated. While akinesia and stationary movement points were confounded. The top and right axes represent states' marginal distribution on Components 1 and 2, respectively. **c. Most important kinematic features.** Permutation test to determine which kinematic features are the most relevant to the distinction between classes. **d. Kinematic scalings.** Visualization of the most relevant kinematic features of the LDA. High values in speed-related variables correlate with the gait state. **e. Confusion Matrix using kinematic features.** Average performance of LDA in a cross-validation design. A linear model trained only on kinematic features could separate the gait state from the states of stationary movement and gait. **f. LDA using neural features.** Using features computed from the ECoG data, points belonging to the akinesia state were minimally separated. Points belonging to stationary movement and gait were confounded. The top and right axes represent states' marginal distribution on Components 1 and 2, respectively. **g. Most important neural features.** Similarly, the permutation test of the neural features revealed the most relevant neural features. The side of the feature is indicated by the letter in parenthesis. **h. Neural scalings.** Visualization of the most relevant neural feature of the LDA. High values of beta band-related features and Hjorth complexity correlated weakly with the akinetic state, and high values of gamma band and Hjorth mobility correlated weakly with the gait state. **i. Confusion Matrix using neural features.** A linear model trained only on neural features can distinguish above chance level the akinetic state from the active states of stationary movement and gait.

Neural Network model refines locomotion states characterization

To account for possible limitations of linear models for non-linear data analysis (*Urai et al. 2022*), we analysed the multimodal dataset using the toolbox CEBRA ("Consistent EmBeddings of high-dimensional Recordings using Auxiliary variables") (*Schneider et al. 2023*), a deep neural network trained using contrastive learning. We computed the low-dimensional embeddings using supervised training for the selection of the contrastive learning sampling and then trained a K-Nearest Neighbors (KNN) classifier to estimate the performance of the model.

Following a similar strategy as for the linear model, we first evaluated the kinematic portion of the features dataset. We projected the kinematic data in a low-dimensional embedding, to visualize the distribution (**Fig 3a**). Then, we assessed the importance of each feature within a cross-validation. We embedded the test dataset, randomizing one feature at a time, and evaluated the embedding with a KNN classifier by computing the f1-score. Calculating the importance score allowed us to estimate what kinematic features are most relevant in constructing the embedding (**Fig 3b**). Once more, linear speed appeared to be the predominant feature category. To inspect how the features mapped into the embedding, we colour-coded each data point in the embedding for the feature amplitude, creating feature heatmaps. (**Fig 3c**, heatmaps of the first 10 features available in **Suppl. Fig 3a**). Finally, we evaluated the performance of the model in classifying unseen data by computing the average confusion matrix (f1-score: 0.87), based on a KNN classifier (**Fig 3d**). The classification score maintained a good level of separation (94% $\pm$8% true positive for the akinetic/stationary group, 83% $\pm$13% true positive for the gait class), greatly improving on the false negative gait state (17% $\pm$13% false negative), at the expense of a small rise in the false positive score (6% $\pm$8% false positive) in comparison to the LDA model (**Fig 3d**), **Suppl. Fig 2a** displays the expanded 3x3 confusion matrix.

Similarly, we reproduced the same pipeline, using the neural portion of the multimodal dataset. We first transformed the data onto a 3D embedding (**Fig 3e**), and visually confirmed a better separation of the states' clusters as was previously achieved by the LDA model (**Fig 2f**). Computing the importance score validated the relevant role played by the frequency-domain feature "gamma amplitude" and the temporal-domain feature "Hjorth complexity" which was previously suggested by the linear model. Features related to the beta band were also retrieved as relevant features (**Fig 3f**). Mapping the values of each parameter onto the data points revealed a cluster of high Hjorth complexity values, in correspondence of the akinetic state, and partially the stationary movement state (**Fig 3g**, heatmaps of the first 10 features available in **Suppl. Fig 3b**). This distribution showed a similar representation as the beta band amplitude feature; in contrast, the gamma power maps with gait and partially stationary movement. Finally, computing the confusion matrix of the classification of unseen data (f1-score:0.73), revealed an improvement in the classification of akinetic states (68% $\pm$9% of true positive for akinetic class and 80% $\pm$7% for the gait/stationary movement group) an improvement in the false negative (32% $\pm$9%) , at the expense of a slight rise in the false positive score (20% $\pm$7%) in comparison to the LDA model (**Fig 3h**), **Suppl. Fig 2b** displays the expanded 3x3 confusion matrix.

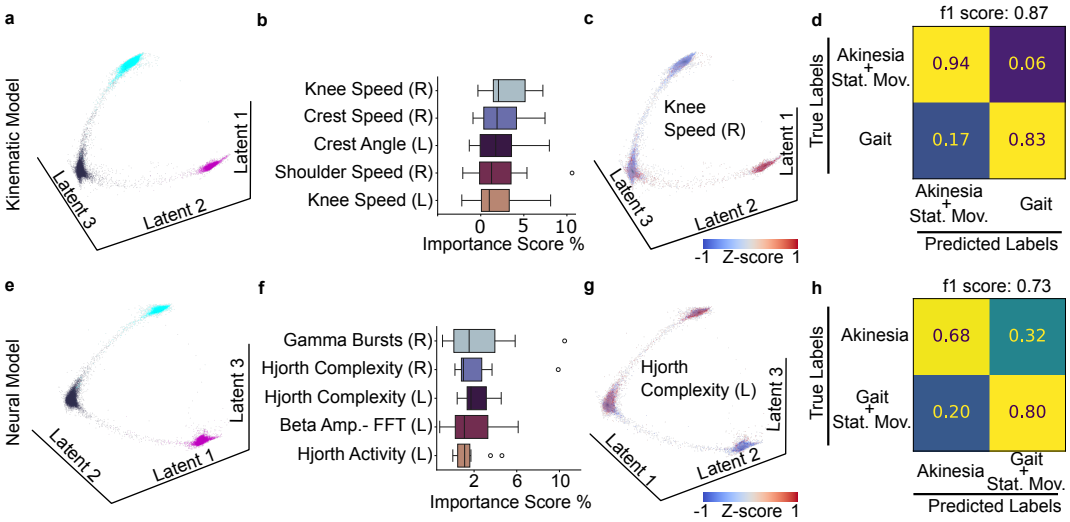

Figure 3. Neural Network model refines locomotion states characterization

a. CEBRA embedding using kinematic features. We trained a supervised CEBRA model to obtain a low-dimensional embedding of datapoints, using the kinematic portion of the multimodal dataset. **b. Most important kinematic features.** The importance score of each feature was evaluated by randomizing one feature at a time and evaluating the resulting embedding with a KNN classifier. **c. Exemplary kinematic feature projection.** To visualize the distribution of features in the embedding, we mapped the value of the features onto each datapoint. Mapping the top-scoring left hip angle value revealed a correlation between higher values and states of akinesia and stationary movement. **d. Confusion Matrix using kinematic features.** We used a KNN classifier to evaluate the average model performance in a cross-validation design. A model using kinematic features allowed the differentiation of the gait from stationary movement and akinesia. **e. CEBRA embedding using neural features.** We trained a supervised CEBRA model to obtain a low-dimensional embedding of datapoints, using the neural portion of the multimodal dataset. **f. Most important neural features.** Importance score was calculated as described for the kinematic features. **g. Exemplary neural feature projection.** Mapping the top-scoring Hjorth Complexity values from the left ECoG onto the datapoints revealed a strong correlation between the feature values and stationary states, specifically akinesia. **h. Confusion Matrix using neural features.** A model using neural features allowed the differentiation of the akinetic state from gait and stationary movement.

Identified neural features associate with akinetic state

Finally, we set to characterize the identified neural features relevant for the separation of locomotion states, and their relationship to akinetic episodes. Plotting each feature as a function of its importance score for the linear and deep-learning models, allowed us to identify consistently high-scoring features: Hjorth complexity (left hemisphere), gamma amplitude (computed with a Fast Fourier Transform (FFT), right hemisphere), Hjorth mobility (right hemisphere) and beta amplitude (computed with an FFT), left hemisphere) (**Fig 4a**). Both beta and gamma features are known correlates of akinetic and prokinetic episodes, respectively (***Tinkhauser et al., 2017***; ***Oehrn et al., 2024***). However, Hjorth's parameters have remained under-explored features. Hjorth complexity and mobility reflect, respectively, the deviation from a pure sine wave, and the average frequency content (**Fig 4**b). Plotting the average temporal modulation of these four features around the onset of (N=75) episodes of akinesia revealed common patterns. Specifically, Hjorth complexity appeared to trace similar temporal profiles as beta amplitude and to undergo a sharp increase at the akinetic episode onset (**Fig 4c**). Conversely, Hjorth mobility displayed a similar profile to gamma amplitude, with a gradual decline preceding and during the akinetic episode onset (**Fig 4d**). We then explored the group-level modulation of these features across locomotion states. We calculated significance with a related t-test ($\alpha < 0.05$), adjusting for multiple comparisons using a Bonferroni-Holm correction (12 tests). Hjorth Complexity was significantly up-modulated specifically during states of akinesia, whereas gamma amplitude demonstrated a down-modulation during episodes of akinesia, in comparison to the gait state (**Fig 4e**). Finally, we qualitatively inspected the ability of beta amplitude or Hjorth complexity to segregate the locomotion states. We computed two embeddings based only on one of the two neural features. Both the data projection in the embedding and the f1-scores (calculated in a cross-validation design) show comparable separation, with a slight advantage of the Hjorth complexity over the beta band-based embedding (**Fig 4f**)

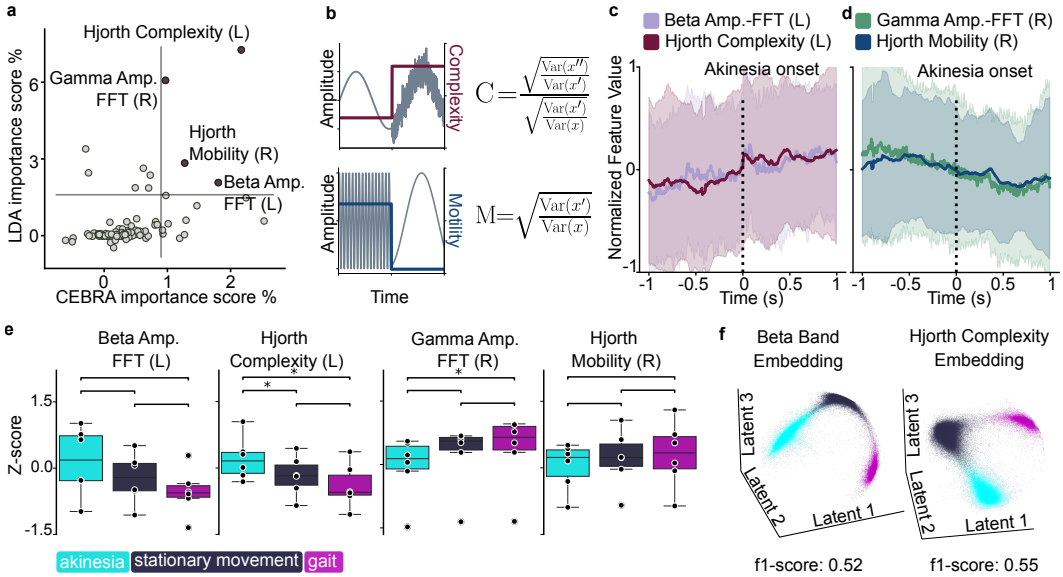

Figure 4. Identified neural features associate with akinetic state

a. Combined LDA and CEBRA importance score. Plotting the importance scores for LDA and the CEBRA model, of each feature, identified features of interest that scored high in both models. **b. Hjorth complexity and motility representation.** The upper panel depicts a mock signal with Hjorth complexity (thick purple line) increasing at the middle point. The lower panel depicts a mock signal with Hjorth mobility (thick blue line) decreasing at the middle point. **c. Hjorth complexity positively correlated with akinetic onset.** Comparison of the average (thick lines) temporal change of the beta band amplitude (a known hallmark of PD) to that of the identified Hjorth complexity. Both displayed a distinct increase at the akinetic state onset. Shades represent the standard deviation **d. Hjorth mobility negatively correlated with akinetic onset.** Comparison of the average (thick lines) temporal change of the gamma band amplitude (a known correlate of prokinetic states) to that of the identified Hjorth mobility. Both displayed a gradual decrease at the akinetic state onset. Shades represent the standard deviation **e. Group comparison of selected features.** Quantification of the selected features at the group level. The Hjorth complexity value was significantly up-modulated during akinesia compared to during stationary movement and gait. The gamma amplitude was significantly down-modulated during akinesia compared to gait. Significance was calculated with a related t-test, adjusted for multiple comparisons with a Bonferroni-Holm correction for 12 tests. **f. Single feature embeddings.** Left: CEBRA embedding created using only the Beta Amplitude - FFT (L) feature. Right: CEBRA embedding created using only the Hjorth Complexity (L) feature. f1-scores are computed in a cross-validation design.

Discussion

In this study we set to discover novel fingerprints of akinetic states, by analysing kinematic and ECoG multimodal data from a Parkinson's rodent model. Additionally, we demonstrated the utility of the open-source package *neurokin*, by relating locomotion states to known neural biomarkers. First, we built a streamlined pipeline using *neurokin* to refine the quantification of previous findings, confirming that parkinsonian animals spend significantly more time in akinesia, during which the beta band power was elevated. Next, we created a neurobehavioural dataset, that captured both the kinematic and neural aspects of locomotion states. We trained a linear model and a neural network on this multimodal dataset, to identify critical neural features characterizing akinetic states. Specifically, our results linked Hjorth complexity and Hjorth mobility to the onset of akinetic episodes. Time-domain biomarkers like Hjorth parameters are appealing for real-time closed-loop stimulation because they bypass the added computational cost and latency of frequency-domain analyses (***Little and Brown 2012***). We propose these novel neural fingerprints as potential biomarkers of akinetic states, which could be further explored as targets for precision interventions such as closed-loop stimulation.

neurokin design and scope

Several toolboxes support the exploration of complex datasets to enable in-depth analysis (***Wiltschko et al. 2015***, ***Viejo et al. 2023***, ***Gramfort 2013***, ***Skrobot et al. 2024***, ***Gill et al. 2020***). Commonly available packages focus on providing data handling platforms or specialized analysis pipelines that rely on pre-processed data. We identified the need for a package capable of managing the import and processing of raw data, accommodating multimodal recording methods, and simultaneously including feature extraction tools.

MNE-Python (***Gramfort, 2013***) is used to analyse human neurophysiological data (MEG, EEG, connectivity, etc.). Although it is comprehensive and effective for high-dimensional, spatially resolved data, it can become overly complex when handling low-dimensional neural data (e.g., fewer 10 ECoG channels). In contrast, we prioritized simplifying data import from prevalent neural recording systems and offered streamlined, modular neural analysis tools.

The toolbox Pynapple (***Viejo et al., 2023***) offers a straightforward method to standardize time-stamped data, alleviating comparable challenges. However, users must pre-process their raw data to ensure compatibility and, although kinematic data can be combined, feature extraction was not supported by default. In contrast, *neurokin* offers user-friendly ways of importing raw data and a customized pipeline for extracting kinematic properties, making it a versatile tool.

The packages MoSeq (***Wiltschko et al., 2015***) and Keypoint-MoSeq also facilitate the discovery of neural correlates. However, they focus on movement motifs that are identified in an unsupervised manner. Our toolbox focuses on the analysis of observed phenotypes, restricting the analysis to pre-labelled data.

We sought to adhere to the FAIR (Findable, Accessible, Interoperable, Reusable) principles (***Barker et al. 2022***). Specifically, *neurokin* was openly available on GitHub (neurokin) and pip installable (pip install neurokin) ("**F**" principle), it includes independent documentation (neurokin documentation) ("**A**" principle), it uses standard domain-relevant file types (e.g., .c3d or .csv) ("**I**" principle), it builds upon qualified software (e.g., numpy, pandas) and details a permissive MIT License ("**R**" principle). Building on these principles, we encourage community-wide code review and participation for further development.

Finally, we designed *neurokin* to provide a bridge between data management and specialized feature research. We envision it to be a helpful toolbox for researchers aiming to collect and analyse with ease multimodal datasets, capturing both the kinematic and neural aspects of their experiments.

Model-based stimulation control

Parkinson's disease was characterized by a heterogeneous symptom distribution (*Moustafa et al. 2016*; *Chaudhuri et al. 2006*; *Kalia and Lang 2015*). While pharmaceuticals and open-loop DBS treatment effectively address symptoms like tremor and bradykinesia, complex manifestations like locomotion disturbances and freezing of gait respond poorly (*Pötter-Nerger and Volkmann 2013*). Closed-loop DBS has been proposed to address these symptoms by adapting the stimulation in real-time. Most adaptive DBS are devised as algorithms proportional to the amplitude of the beta band (*Tinkhauser et al. 2017*), however these therapy strategies have yet to reach optimal results (*Pozzi et al. 2022*). Moreover, calculating features in the frequency domain or through filtering introduces lags that can delay an effective intervention. Additionally, an ideal therapy should be tailored to the specific subset of symptoms that a patient displays, thus maximizing the benefits while minimizing adverse effects. Thus, finding a range of computationally lightweight features, that can be combined in a model-based control (*Little and Brown, 2012*) and can reliably detect a pathological state will be crucial to develop personalized stimulation strategies to mitigate, or avoid altogether a pathological motor state. Finding a feature vector that allows to identify a pathological state, can be conceived as discovering its fingerprint, which, eventually, could be target it with a timely neuromodulation. Ultimately, we envision a closed-loop algorithm based on real-time mapping of the neural state projected to a patient-specific embedding. This tailored neural projection would reveal the transitions into pathological states and guide targeted interventions to relieve or avoid pathological manifestations altogether (**Video supplement 2** illustrates an offline proof of concept of neural state tracking in a neural embedding).

Refined characterization of locomotion states in a Parkinson's rodent model

In this study, we first validated our model to be suitable in quantifying locomotion deficits and to exhibit known neural correlates. Indeed we confirmed that PD animals spent significantly less time in gait and more in akinetic episodes, compared to sham controls. This aligns with results obtained in *Xiao et al. 2017*, which highlighted an enhanced time spent in immobility, in a comparable animal model. Next, we highlighted a significant increase in the beta power, particularly in the state of akinesia. Then we sought to identify additional biomarkers that could serve as putative targets for DBS, using linear and non-linear models.

We retrieved known correlates of akinesia and bradykinesia such as beta band amplitude (*Brown 2007*, *Lofredi et al. 2019*), as well as known correlates of prokinetic activity such as gamma band amplitude (*Litvak et al. 2012*), thereby corroborating the validity of our method. Interestingly, less explored but promising (*Lee et al. 2022*) features such as Hjorth complexity and mobility were also significantly modulated. Hjorth parameters were first established to quantify EEG traces, and provide a bridge between the time domain and the conventionally analysed frequency domain (*Hjorth 1970*). Since then, they have been explored as biomarkers to classify Alzheimer's Disease patients (*Safi and Safi 2021*, *Puri et al. 2025*), and Parkinson's Disease patients (*Coelho et al. 2023*). Here we established that Hjorth parameters are predictive of Parkinsonian disease states in a rodent model, and uncovered the specific modulation of the complexity and mobility parameters at the onset of akinesia. Employing them — either alone or in combination — could improve early detection of akinetic states during locomotion and enable interventions tailored to each patient's clinical profile. By offering low-latency, physiologically relevant markers, these features represent a promising step toward more effective, symptom-specific DBS protocols.

Limitations and outlook

While *neurokin* can empower the discovery of locomotion neural correlates, the package comes with some limitations. Mainly, the current version supports a limited set of recording systems. However, the modular design of neurokin allows for an easy expansion to support additional recording setups Moreover, the open-source nature of the package invites community contributions that will

enrich the set of input data supported, including for human analysis. Therefore the toolbox might help aligning movement research across species. The analysis presented in this study was focused on three locomotor behaviours (akinesia, stationary movement, and gait) that were clearly recognizable during the runway task. It is notable that both the linear and non-linear kinematic models could not perfectly separate the akinetic state from the stationary movement. However, this is explainable as no markers were placed on the forelimb or on the head of the animals, which often remained the only body parts active during stationary movement. So, while the akinetic state was apparent from the video recording (used to create the ground-truth labels), it was challenging to distinguish from the available 3D coordinates. Further analyses of this Parkinson's model could include other behavioural states, and potentially lead to the uncovering of additional neural correlates of the disease. Nevertheless, the pipeline established here could serve as a template to explore other states, as well as the effects of treatments (e.g., pharmaceuticals, electro- or optostimulation) on neural correlates.

In the future, the neural correlates uncovered in this study may prove to be novel targets for a closed-loop stimulation that adapts in real-time to the current locomotor state, providing an on-demand delivery method.

Methods and Materials

neurokin's modular and open-source design

We developed neurokin, a platform to streamline the integration of three distinct types of data: neural local field potentials, kinematic recordings, and event labels. The package was primarily object-oriented, to ensure a coherent interface across data types. The underlying principle of *neurokin* was modularity, both enabling the use of any of the classes independently (to facilitate data import and management), and supporting the assembling of project-specific pipelines. Moreover, *neurokin* adheres to the FAIR principles.

Kinematic data

This class handles 2D and 3D kinematic data originating from optoelectrical gait systems such as Vicon (.c3d file format), or files from computer vision toolboxes (e.g., DeepLabCut). Upon importing the data in the corresponding kinematic object, the user can make use of the kinematic-features extraction pipeline. This pipeline was designed to maximize flexibility. To this end, the user can define a custom skeleton via a configuration file, and select standard features (e.g., speed, acceleration, height). Additionally, the framework supports the straightforward addition of custom features.

Neural data

This class operates on neural recordings, such as ECoG and Local Field Potentials (LFPs), standardising data from different recording systems in a common format to interface with fundamental methods (e.g., timestamps-parsing, PSD calculation). It was currently compatible with the Tucker-Davis Technologies apparatus and OpenEphys data, with the possibility to be expanded to other hardware.

Events data

Users can define the events by providing labels. These are used to retrieve corresponding kinematic and neural data, and can eventually be used as inputs for machine learning applications. We tailored a pipeline to retrieve Vicon labels and align them with kinematic and neural features. This can easily be expanded to support any time-stamped, user-defined events.

Animal Model and Surgical Procedures

All experiments were conducted in accordance with the German regulatory body (LaGeSo), specifically under the animal licence number G0206/19. Experiments were performed on male Sprague

Dawley rats with initial weights of 200-250 g, ordered from Janvier Labs. Animals were kept in a 12-hour light cycle with ad-libitum access to food and water.

All the interventions were performed under full general anaesthesia with isoflurane (1–2%) in oxygen-enriched air. After surgery, the rats were placed in an incubator for optimised recovery from anaesthesia as described in ***Wenger et al. 2016***.

PD models were injected with 6-OHDA (Sigma: H4381) dissolved immediately before use in a buffer solution of 0.02% w/v ascorbic acid achieving a final concentration of 8 mg/mL. Of the 6-OHDA solution 1.2 μL was injected at a rate of 0.04 mL/min through a pipette according to ***McNamara et al. 2022***. Shams were injected with the same solution except for 6-OHDA. The injection was targeted to the Medial Forebrain Bundle (coordinates from bregma: AP: -2.6 mm, ML: 1.6 mm, DV: -8.4 mm from skull surface). The success of the 6-OHDA model was verified with the antibodies anti-tyrosine hydroxylase (abcam: ab112) and anti-rabbit Alexa 488 (Thermofisher: A-11034).

Following a recovery period of 2 weeks, the rats were implanted with 2 stainless steel ECoG screws (2 mm) over the motor cortex (left and right hemisphere), one ground screw over the cerebellum, and 2 LFP probes targeted to the STN area (left and right hemisphere). No data from the LFP electrodes was analyzed in this study.

To guarantee the protection of the implant, we designed a three component cap, that can be 3D printed and assembled during surgery. The 3D-printing files are openly available (headstage caps).

Runway Task

We trained the rats to run from one end of a 15x140 cm runway to the other. We placed a cage with at least one additional rat at the end of the runway to further motivate the tested rat. At the beginning of each recording the rat was placed at the starting end of the runway, then given up to a minute to spontaneously initiate walking. If, by the end of the given time, the rat had not run the whole length, it was gently brought to the ending side for a few seconds while the recording setup was prepared for the next recording. This ensured exposure to the additional rats and minimized idle time at the starting point. We repeated the task until 15 successful crossings were achieved, or the total recording time per animal reached 20 minutes. To ensure consistency across sessions, we marked with a permanent marker the joint points (shoulder, iliac crest, hip, knee, ankle, and metatarsophalangeal joint) on the skin. Then, at the start of each session, 4 mm reflective markers were glued with double-sided tape on the marked spots.

Kinematic Data Recording

To capture the movements of the rats we used an infrared camera-based motion capture system (Vicon). We equipped a 2.5 m2 room with 10 infrared and 2 HD wall-mounted cameras. The infrared cameras were positioned around 3 sides of the runway covering different heights. Data from the infrared cameras was recorded at a sampling rate of 200 Hz, and videos from the HD cameras were recorded at 50 Hz. The raw data was then processed using the Nexus software (v2.12.1). Each recording was cropped from the earliest point where all the markers were visible and no contact between the experimenter and the animal was observed, to the last point where the markers were visible and no contact with the experimenter was observed, or to the end of the run. The 3D position of each joint was manually reconstructed using a custom-defined bipedal skeleton (as no markers were placed on the forepaws). The data was then exported in the .c3d format.

Neural Data Recording

To record ECoG neural signals we used stainless steel screws (DIN 84 A2 M1.2x2 from MaxWitte GmbH), laser soldered to a 10T stainless steel PFA-coated wire (SS-10T/A from Science Products). The wires, soldered to Omnetics 32-channel connectors, were coated with Epoxy resin, to grant stability and all the unused channels were shorted to the ground. During experiments, we plugged a digitising headstage (Intan), to minimise movement artefact and used a TDT recording apparatus.

The signal pipeline was then controlled through the software Synapse. We recorded all raw data at a sampling frequency of 24414.1 Hz, data from implanted LFP electrodes were not analysed.

Locomotion State Labelling

We defined akinesia on a phenotypic level, observing an almost complete lack of any type of movement. This was to be contrasted with stationary movement, where the rat was in an engaged state and performing an array of behaviours (e.g., grooming or sniffing) and gait, when the rat was walking. The events, were manually labelled in the Nexus software. The data was then exported in the ASCII format to a .csv file.

Locomotion State Distribution Analysis

We used *neurokin* to process the .csv files generated by the Nexus software, and created a dataset summarizing all the events timestamps in each run. For each run, we computed the percentage of time spent in each locomotion state. Next, we computed subject-level averages and quantified the differences in locomotion state distribution between the sham control and the PD animals. We performed an independent t-test with a Bonferroni-Holm correction for multiple comparisons (3 comparisons). We assumed an α<0.05.

Kinematic Features Dataset Creation

To create the neural and kinematic dataset we relied on a consistent folder structure that was then automatically processed. We used *neurokin* to import and process the .c3d and .csv files generated by Vicon. We selected kinematic features representing speed, acceleration, angle variation for the various markers, forward movement and height for the metatarsophalangeal joint. We based our feature extraction on a sliding-window strategy. The kinematic features were computed at a 200 Hz rate (i.e., 5 ms window with a 2.5 ms overlap with the following window).

Neural Features Dataset Creation

Using *neurokin*, we selected the neural data corresponding to the valid portion of the recording (all markers visible, no contact with the experimenter). To extract neural features we relied on the package *py_neuromodulation* (***Merk et al., 2023***), and used a feature sampling rate of 200 Hz, thus aligning with the kinematic features framerate. We computed 108 parameters, among which temporal features (e.g., Hjorth parameters), oscillatory features (e.g., power of the beta band and gamma band) and waveform shapes (e.g., sharp wave intervals). In rare occasions, we encountered a length mismatch between the kinematic and the neural files. Upon reviewing the original files, we discovered that seldomly a few additional frames were recorded at the beginning of the kinematic file, we discarded files with excessive length mismatch, and trimmed those with minimal mismatch (typically 1-2 frames).

Multimodal Dataset Creation and Testing Parameters

For each of the valid runs, we filtered for outliers (set to median value) and Z-scored column-wise. Finally, we concatenated all runs in a multimodal (kinematics, neural and labels) dataset. To validate the model, we performed an 11-fold cross-validation - as 55 runs were present, at each iteration we trained on 50 runs and tested on 5 unseen ones. We used random seeds to ensure all analyses were done on the same splits.

LDA analysis

The visualization of the entire model was achieved by training and transforming the whole dataset and computing kernel density estimation marginal distributions. Importance scores were computed for each feature, for each fold of the cross-validation, using the *sklearn* package (***Pedregosa et al., 2011***), specifically calculating the balanced accuracy. The final confusion matrix was calculated as the average of the 11 folds.

CEBRA analysis

We used a CEBRA model (***Schneider et al., 2023***) with the following parameters: *model_architecture* = “offset200-model”, *batch_size* = 512, *temperature* = 0.1 (value set after temperature optimization scan), *learning_rate* = 0.0005, *max_iterations* = 50000, *time_offsets* = 200, *output_dimension* = 3, *conditional* = “time_delta”. This allowed us to use the state labels as the categorical variable used to optimize the contrastive learning steps. The "offset200-model" was custom made to have a receptive field of 200 samples, corresponding to 1s of data. To evaluate the performance of the model we used a KNN decoder with *n_neighbors* = 3 and *metric* = "cosine". Importance scores were computed for each feature, for each fold of the cross-validation, using the *f1_score* calculation from the *sklearn* package. The final confusion matrix was calculated as the average of the 11 folds.

Statistical Analysis of Selected Features Alignment

The significance of each selected feature, was computed as a related t-test between the compared state. To correct for multiple comparisons, we used a Bonferroni-Holm correction, ranking 12 t-test (3 states, 4 features). We assumed an α<0.05.

Acknowledgments

Computation has been performed on the HPC for Research/Clinic cluster of the Berlin Institute of Health. We thank Gianni Garulli for help in developing the 3D-printable recording cap. We thank the Scientific Laboratories Center at Charité for 3D-printing services. We thank Dipl.-Ing. Raik Paulat for technical support and set-up of the recording room. E.L.G., T.M., B.K., D.D., W.J.N., Y.P., M.E., C.H. and N.K. received funding from Collaborative Research Center ReTune TRR 295-424778381. W.J.N. received funding from the European Union (ERC, ReinforceBG, project 101077060), and the Bundesministerium für Bildung und Forschung (BMBF, project FKZ01GQ1802). M.E. received funding from DFG under Germany´s Excellence Strategy – EXC-2049 – 390688087, Clinical Research Group KFO 5023 BeCAUSE-Y, project 2 EN343/16-1. BMBF, DZNE, DZHK, DZPG, EU, Corona Foundation, and Fondation Leducq. C.H. received funding from DFG under Germany´s Excellence Strategy – EXC-2049 – 390688087 (SPARK-BIH Stroke Protect), EraNet Neuron project DFG project number 522473931, DZHK/BMBF Innovation Cluster (FKZ81X2100285), Charité 3R (C3RHeaD and STROKE-PREDICT-C3R), BIH, and Fondation Leducq Transatlantic Network of Excellence (17CDV03).

Conflict of Interest

WJN received honoraria for consulting from InBrain – Neuroelectronics that is a neurotechnology company and honoraria for talks from Medtronic that is a manufacturer of deep brain stimulation devices unrelated to this manuscript.

Ethics approval

All experiments were conducted in accordance with the German regulatory body (LaGeSo) under the animal licence number G0206/19.

Data availability

The full dataset analysed in this manuscript is published with the DOI: **10.5281/zenodo.15163493**. 3D models of the recording cap are available on GitHub (headstage caps)

Code availability

The code used to perform all the analysis in this manuscript is available in the akinesia_fingerprint_article repository. The *neurokin* toolbox is available on GitHub (neurokin) and pip installable (pip install neurokin).

References

Barker M, Chue Hong NP, Katz DS, Lamprecht AL, Martinez-Ortiz C, Psomopoulos F, Harrow J, Castro LJ, Gruenpeter M, Martinez PA, Honeyman T. Introducing the FAIR Principles for research software. Scientific Data. 2022 Oct; 9(1). http://dx.doi.org/10.1038/s41597-022-01710-x, doi: 10.1038/s41597-022-01710-x.

Brazhnik E, Novikov N, McCoy AJ, Cruz AV, Walters JR. Functional correlates of exaggerated oscillatory activity in basal ganglia output in hemiparkinsonian rats. Experimental Neurology. 2014; 261:563–577. https://www.sciencedirect.com/science/article/pii/S0014488614002386, doi: https://doi.org/10.1016/j.expneurol.2014.07.010.

Brown P. Abnormal oscillatory synchronisation in the motor system leads to impaired movement. Current Opinion in Neurobiology. 2007 Dec; 17(6):656–664. http://dx.doi.org/10.1016/j.conb.2007.12.001, doi: 10.1016/j.conb.2007.12.001.

Castrioto A. Ten-Year Outcome of Subthalamic Stimulation in Parkinson Disease: A Blinded Evaluation. Archives of Neurology. 2011 Dec; 68(12):1550. http://dx.doi.org/10.1001/archneurol.2011.182, doi: 10.1001/archneurol.2011.182.

Chaudhuri KR, Healy DG, Schapira AH. Non-motor symptoms of Parkinson's disease: diagnosis and management. The Lancet Neurology. 2006 Mar; 5(3):235–245. http://dx.doi.org/10.1016/S1474-4422(06)70373-8, doi: 10.1016/s1474-4422(06)70373-8.

Coelho BFO, Massaranduba ABR, Souza CAdS, Viana GG, Brys I, Ramos RP. Parkinson's disease effective biomarkers based on Hjorth features improved by machine learning. Expert Systems with Applications. 2023 Feb; 212:118772. http://dx.doi.org/10.1016/j.eswa.2022.118772, doi: 10.1016/j.eswa.2022.118772.

Degos B, Deniau JM, Chavez M, Maurice N. Chronic but not acute dopaminergic transmission interruption promotes a progressive increase in cortical beta frequency synchronization: relationships to vigilance state and akinesia. Cereb Cortex. 2009 Jul; 19(7):1616–1630.

Gill JP, Garcia S, Ting LH, Wu M, Chiel HJ. neurotic: Neuroscience Tool for Interactive Characterization. eneuro. 2020 Apr; 7(3):ENEURO.0085–20.2020. http://dx.doi.org/10.1523/ENEURO.0085-20.2020, doi: 10.1523/eneuro.0085-20.2020.

Gramfort A. MEG and EEG data analysis with MNE-Python. Frontiers in Neuroscience. 2013; 7. http://dx.doi.org/10.3389/fnins.2013.00267, doi: 10.3389/fnins.2013.00267.

Hjorth B. EEG analysis based on time domain properties. Electroencephalography and Clinical Neurophysiology. 1970; 29(3):306–310. https://www.sciencedirect.com/science/article/pii/0013469470901434, doi: https://doi.org/10.1016/0013-4694(70)90143-4.

Kalia LV, Lang AE. Parkinson's disease. The Lancet. 2015 Aug; 386(9996):896–912. http://dx.doi.org/10.1016/S0140-6736(14)61393-3, doi: 10.1016/s0140-6736(14)61393-3.

Kiehn O. Decoding the organization of spinal circuits that control locomotion. Nature Reviews Neuroscience. 2016 Mar; 17(4):224–238. http://dx.doi.org/10.1038/nrn.2016.9, doi: 10.1038/nrn.2016.9.

Kranick SM, Hallett M. Neurology of volition. Experimental Brain Research. 2013 Jan; 229(3):313–327. http://dx.doi.org/10.1007/s00221-013-3399-2, doi: 10.1007/s00221-013-3399-2.

Latash ML. 11 - Exemplary behaviors. In: Latash ML, editor. *Fundamentals of Motor Control* San Diego: Academic Press; 2012.p. 211–259. https://www.sciencedirect.com/science/article/pii/B9780124159563000117, doi: https://doi.org/10.1016/B978-0-12-415956-3.00011-7.

Lee SB, Kim YJ, Hwang S, Son H, Lee SK, Park KI, Kim YG. Predicting Parkinson's disease using gradient boosting decision tree models with electroencephalography signals. Parkinsonism & Related Disorders. 2022 Feb; 95:77–85. http://dx.doi.org/10.1016/j.parkreldis.2022.01.011, doi: 10.1016/j.parkreldis.2022.01.011.

Little S, Brown P. What brain signals are suitable for feedback control of deep brain stimulation in Parkinson's disease? Annals of the New York Academy of Sciences. 2012 Jul; 1265(1):9–24. http://dx.doi.org/10.1111/j.1749-6632.2012.06650.x, doi: 10.1111/j.1749-6632.2012.06650.x.

Little S, Pogosyan A, Neal S, Zavala B, Zrinzo L, Hariz M, Foltynie T, Limousin P, Ashkan K, FitzGerald J, Green AL, Aziz TZ, Brown P. Adaptive deep brain stimulation in advanced Parkinson disease. Annals of Neurology. 2013 Jul; 74(3):449–457. http://dx.doi.org/10.1002/ana.23951, doi: 10.1002/ana.23951.

Litvak V, Eusebio A, Jha A, Oostenveld R, Barnes G, Foltynie T, Limousin P, Zrinzo L, Hariz MI, Friston K, Brown P. Movement-Related Changes in Local and Long-Range Synchronization in Parkinson's Disease Revealed by Simultaneous Magnetoencephalography and Intracranial Recordings. Journal of Neuroscience. 2012 Aug; 32(31):10541–10553. http://dx.doi.org/10.1523/JNEUROSCI.0767-12.2012, doi: 10.1523/jneurosci.0767-12.2012.

Lofredi R, Tan H, Neumann WJ, Yeh CH, Schneider GH, Kühn AA, Brown P. Beta bursts during continuous movements accompany the velocity decrement in Parkinson's disease patients. Neurobiology of Disease. 2019 Jul; 127:462–471. http://dx.doi.org/10.1016/j.nbd.2019.03.013, doi: 10.1016/j.nbd.2019.03.013.

Martínez-Fernández R, Schmitt E, Martinez-Martin P, Krack P. The hidden sister of motor fluctuations in Parkinson's disease: A review on nonmotor fluctuations. Movement Disorders. 2016 Jul; 31(8):1080–1094. http://dx.doi.org/10.1002/mds.26731, doi: 10.1002/mds.26731.

McNamara CG, Rothwell M, Sharott A. Stable, interactive modulation of neuronal oscillations produced through brain-machine equilibrium. Cell Reports. 2022 Nov; 41(6):111616. http://dx.doi.org/10.1016/j.celrep.2022.111616, doi: 10.1016/j.celrep.2022.111616.

Merk T, Köhler R, Peterson V, Lyra L, Vanhoecke J, Chikermane M, Binns T, Li N, Walton A, Bush A, Sisterson N, Busch J, Lofredi R, Habets J, Huebl J, Zhu G, Yin Z, Zhao B, Merkl A, Bajbouj M, et al. Invasive neurophysiology and whole brain connectomics for neural decoding in patients with brain implants. Res Sq. 2023 Sep; .

Moustafa AA, Chakravarthy S, Phillips JR, Gupta A, Keri S, Polner B, Frank MJ, Jahanshahi M. Motor symptoms in Parkinson's disease: A unified framework. Neuroscience & Biobehavioral Reviews. 2016; 68:727–740. https://www.sciencedirect.com/science/article/pii/S0149763415300919, doi: https://doi.org/10.1016/j.neubiorev.2016.07.010.

Neumann WJ, Turner RS, Blankertz B, Mitchell T, Kühn AA, Richardson RM. Toward Electrophysiology-Based Intelligent Adaptive Deep Brain Stimulation for Movement Disorders. Neurotherapeutics. 2019 Jan; 16(1):105–118. http://dx.doi.org/10.1007/s13311-018-00705-0, doi: 10.1007/s13311-018-00705-0.

Neumann W, Gilron R, Little S, Tinkhauser G. Adaptive Deep Brain Stimulation: From Experimental Evidence Toward Practical Implementation. Movement Disorders. 2023 May; 38(6):937–948. http://dx.doi.org/10.1002/mds.29415, doi: 10.1002/mds.29415.

Nishimaru H, Matsumoto J, Setogawa T, Nishijo H. Neuronal structures controlling locomotor behavior during active and inactive motor states. Neuroscience Research. 2023; 189:83–93. https://www.sciencedirect.com/science/article/pii/S0168010222003017, doi: https://doi.org/10.1016/j.neures.2022.12.011.

Nutt JG, Bloem BR, Giladi N, Hallett M, Horak FB, Nieuwboer A. Freezing of gait: moving forward on a mysterious clinical phenomenon. The Lancet Neurology. 2011 Aug; 10(8):734–744. http://dx.doi.org/10.1016/S1474-4422(11)70143-0, doi: 10.1016/s1474-4422(11)70143-0.

Oehrn CR, Cernera S, Hammer LH, Shcherbakova M, Yao J, Hahn A, Wang S, Ostrem JL, Little S, Starr PA. Chronic adaptive deep brain stimulation versus conventional stimulation in Parkinson's disease: a blinded randomized feasibility trial. Nature Medicine. 2024 Aug; 30(11):3345–3356. http://dx.doi.org/10.1038/s41591-024-03196-z, doi: 10.1038/s41591-024-03196-z.

Oliveira AM, Coelho L, Carvalho E, Ferreira-Pinto MJ, Vaz R, Aguiar P. Machine learning for adaptive deep brain stimulation in Parkinson's disease: closing the loop. Journal of Neurology. 2023 Aug; 270(11):5313–5326. http://dx.doi.org/10.1007/s00415-023-11873-1, doi: 10.1007/s00415-023-11873-1.

Pedregosa F, Varoquaux G, Gramfort A, Michel V, Thirion B, Grisel O, Blondel M, Prettenhofer P, Weiss R, Dubourg V, Vanderplas J, Passos A, Cournapeau D, Brucher M, Perrot M, Duchesnay E. Scikit-learn: Machine Learning in Python. Journal of Machine Learning Research. 2011; 12:2825–2830.

Pötter-Nerger M, Volkmann J. Deep brain stimulation for gait and postural symptoms in Parkinson's disease. Movement Disorders. 2013 Sep; 28(11):1609–1615. http://dx.doi.org/10.1002/mds.25677, doi: 10.1002/mds.25677.

Pozzi NG, Palmisano C, Reich MM, Capetian P, Pacchetti C, Volkmann J, Isaias IU. Troubleshooting Gait Disturbances in Parkinson's Disease With Deep Brain Stimulation. Frontiers in Human Neuroscience. 2022 May; 16. http://dx.doi.org/10.3389/fnhum.2022.806513, doi: 10.3389/fnhum.2022.806513.

Puri DV, Gawande JP, Kachare PH, Al-Shourbaji I. Optimal time-frequency localized wavelet filters for identification of Alzheimer's disease from EEG signals. Cognitive Neurodynamics. 2025 Jan; 19(1). http://dx.doi.org/10.1007/s11571-024-10198-7, doi: 10.1007/s11571-024-10198-7.

Safi MS, Safi SMM. Early detection of Alzheimer's disease from EEG signals using Hjorth parameters. Biomedical Signal Processing and Control. 2021 Mar; 65:102338. http://dx.doi.org/10.1016/j.bspc.2020.102338, doi: 10.1016/j.bspc.2020.102338.

Schneider S, Lee JH, Mathis MW. Learnable latent embeddings for joint behavioural and neural analysis. Nature. 2023 May; 617(7960):360–368. http://dx.doi.org/10.1038/s41586-023-06031-6, doi: 10.1038/s41586-023-06031-6.

Shine JM, Handojoseno AMA, Nguyen TN, Tran Y, Naismith SL, Nguyen H, Lewis SJG. Abnormal patterns of theta frequency oscillations during the temporal evolution of freezing of gait in Parkinson's disease. Clinical Neurophysiology. 2014 Mar; 125(3):569–576. http://dx.doi.org/10.1016/j.clinph.2013.09.006, doi: 10.1016/j.clinph.2013.09.006.

Skrobot M, Sa RD, Walter J, Vogt A, Paulat R, Lips J, Mosch L, Mueller S, Dominiak S, Sachdev R, Boehm-Sturm P, Dirnagl U, Endres M, Harms C, Wenger N. Refined movement analysis in the staircase test reveals differential motor deficits in mouse models of stroke. Journal of Cerebral Blood Flow & Metabolism. 2024 May; 44(9):1551–1564. http://dx.doi.org/10.1177/0271678X241254718, doi: 10.1177/0271678x241254718.

Tinkhauser G, Pogosyan A, Little S, Beudel M, Herz DM, Tan H, Brown P. The modulatory effect of adaptive deep brain stimulation on beta bursts in Parkinson's disease. Brain. 2017 Feb; 140(4):1053–1067. http://dx.doi.org/10.1093/brain/awx010, doi: 10.1093/brain/awx010.

Toledo JB, López-Azcárate J, Garcia-Garcia D, Guridi J, Valencia M, Artieda J, Obeso J, Alegre M, Rodriguez-Oroz M. High beta activity in the subthalamic nucleus and freezing of gait in Parkinson's disease. Neurobiology of Disease. 2014 Apr; 64:60–65. http://dx.doi.org/10.1016/j.nbd.2013.12.005, doi: 10.1016/j.nbd.2013.12.005.

Tovote P. The origins of freezing. Nature Reviews Neuroscience. 2024 Sep; 25(11):709–709. http://dx.doi.org/10.1038/s41583-024-00857-3, doi: 10.1038/s41583-024-00857-3.

Urai AE, Doiron B, Leifer AM, Churchland AK. Large-scale neural recordings call for new insights to link brain and behavior. Nature Neuroscience. 2022 Jan; 25(1):11–19. http://dx.doi.org/10.1038/s41593-021-00980-9, doi: 10.1038/s41593-021-00980-9.

Viejo G, Levenstein D, Carrasco SS, Mehrotra D, Mahallati S, Vite GR, Denny H, Sjulson L, Battaglia FP, Peyrache A. Pynapple, a toolbox for data analysis in neuroscience. eLife. 2023 Aug; http://dx.doi.org/10.7554/eLife.85786.2, doi: 10.7554/elife.85786.2.

Weintraub D, Burn DJ. Parkinson's disease: The quintessential neuropsychiatric disorder. Movement Disorders. 2011 May; 26(6):1022–1031. http://dx.doi.org/10.1002/mds.23664, doi: 10.1002/mds.23664.

Wenger N, Moraud EM, Gandar J, Musienko P, Capogrosso M, Baud L, Le Goff CG, Barraud Q, Pavlova N, Dominici N, Minev IR, Asboth L, Hirsch A, Duis S, Kreider J, Mortera A, Haverbeck O, Kraus S, Schmitz F, DiGiovanna J, et al. Spatiotemporal neuromodulation therapies engaging muscle synergies improve motor control after spinal cord injury. Nature Medicine. 2016 Jan; 22(2):138–145. http://dx.doi.org/10.1038/nm.4025, doi: 10.1038/nm.4025.

Wenger N, Vogt A, Skrobot M, Garulli EL, Kabaoglu B, Salchow-Hömmen C, Schauer T, Kroneberg D, Schuhmann MK, Ip CW, Harms C, Endres M, Isaias IU, Tovote P, Blum R. Rodent models for gait network disorders in Parkinson's disease – a translational perspective. Experimental Neurology. 2022; 352:114011. https://www.sciencedirect.com/science/article/pii/S001448862200036X, doi: https://doi.org/10.1016/j.expneurol.2022.114011.

Wiltschko A, Johnson M, Iurilli G, Peterson R, Katon J, Pashkovski S, Abraira V, Adams R, Datta S. Mapping Sub-Second Structure in Mouse Behavior. Neuron. 2015 Dec; 88(6):1121–1135. http://dx.doi.org/10.1016/j.neuron.2015.11.031, doi: 10.1016/j.neuron.2015.11.031.

Xiao H, Li M, Cai J, Li N, Zhou M, Wen P, Xie Z, Wang Q, Chang J, Zhang W. Selective cholinergic depletion of pedunculopontine tegmental nucleus aggravates freezing of gait in parkinsonian rats. Neuroscience Letters. 2017; 659:92–98. https://www.sciencedirect.com/science/article/pii/S0304394017306638, doi: https://doi.org/10.1016/j.neulet.2017.08.016.